0026-895X/02/6101-136–141$3.00
MOLECULAR PHARMACOLOGY
Vol. 61, No. 1
991/951371
Mol Pharmacol 61:136–141, 2002
Printed in U.S.A.

Structural Basis of Differences in Isoform-Specific Gating and Lidocaine Block between Cardiac and Skeletal Muscle Sodium Channels

RONALD A. LI, IRENE L. ENNIS, GORDON F. TOMASELLI, and EDUARDO MARBÁN

Institute of Molecular Cardiobiology, the Johns Hopkins University School of Medicine, Baltimore, Maryland

Received March 28, 2001; accepted September 28, 2001

This paper is available online at http://molpharm.aspetjournals.org

ABSTRACT

Voltage-gated Na^+ channels underlie rapid conduction in heart and skeletal muscle. Cardiac sodium channels open and close over more negative potentials than do skeletal muscle sodium channels; heart channels are also more sensitive to lidocaine block. The structural basis of these differences is poorly understood. We mutated nine isoform-specific μ1 (rat skeletal muscle) channel residues in domain IV to those at equivalent locations in hH1 (human cardiac) channels. Channel constructs were expressed in tsA-201 cells and screened for changes in gating and lidocaine sensitivity. Only L1373E, located in the linker between the S1 and S2 transmembrane segments, shifted activation gating and use-dependent block by lidocaine toward that seen in hH1. The converse mutation, hH1-E1555L, shifted the phenotype of hH1 to resemble that of μ1. Therefore, we identified a previously unsuspected glutamate-to-leucine isoform-specific variant site (i.e., 1555 in hH1 and 1373 in μ1) that significantly influences gating and drug block in sodium channels. The identification of the residue at this position plays a major role in shaping the responses of sodium channels to voltage and to lidocaine, helping to rationalize the distinctive behavior of cardiac sodium channels.

Despite nearly identical selectivity profiles, sodium channels from different tissues differ greatly in their gating and pharmacological properties. Two such differences are particularly important for cardiac physiology. First, the cardiac Na^+ current activates ~20 mV more negatively than does that of skeletal muscle (Nuss et al., 1995). Second, heart channels are more sensitive than their muscle and nerve counterparts to block by antiarrhythmic drugs such as lidocaine (Nuss et al., 1995; Wang et al., 1996; Makielski et al., 1999). Recent studies have suggested that cytoplasmic channel structures (Bennett, 1999) and glycosylation (Zhang et al., 1999) may play a role in the gating differences between channel isoforms. Local anesthetics (LAs) are known to exert their clinical effects by binding preferentially to inactivated Na^+ channels, which is the channel conformation that accumulates during rapid repetitive activity (Courtney, 1975; Hille, 1977; Hondeghem and Katzung, 1977). The enhanced drug sensitivity of the cardiac channels may simply reflect the fact that the inactivated conformation predominates under physiological conditions (Wright et al., 1997). Alternatively, cardiac channels may bind LAs with an intrinsically higher affinity (Nuss et al., 1995; Wang et al., 1996). In any case, the mechanisms of these isoform-specific differences in gating and drug sensitivity remain poorly defined.

Because channel activation is known to involve substantial charge movements (Stühmer et al., 1989; Sigworth, 1993; Chahine et al., 1994; Yang et al., 1996), we first compared the amino acid sequences of μ1 (rat skeletal muscle) and hH1 (human heart) channels and sought differences in charged residues in domain IV (DIV). The initial focus was placed on this domain because it plays a unique role in channel activation, inactivation, and the molecular coupling between these processes (Chahine et al., 1994; Chen et al., 1996; Yang et al., 1996). DIV also contains residues that are known to influence LA block (Ragsdale et al., 1994, 1996). Sequence alignment revealed four charge differences [i.e., S1/2-L1373(E), S2-D1376(N), S2-N1380(K), and S5-K1502(W), and numbering was taken from the μ1 sequence with residues at equivalent locations in hH1 in parentheses; Fig. 1]. Although these residues are not located within the S4 "voltage sensor", they may interact electrostatically and/or chemically with S4 residues, thereby influencing channel activation. Indeed, charged residues other than those in the S4

This work was supported by National Institutes of Health Grants R01-HL52768 (to E.M.) and R01-HL50411 (to G.F.T.), by a Research Career Development Award from the Cardiac Arrhythmias Research & Education (CARE) Foundation, Inc. (to R.A.L.), and by a fellowship award from Fondo para el Mejoramiento de la Educación, Argentina (I.L.E.). E.M. holds the Michel Mirowski, M.D., Professorship of Cardiology at The Johns Hopkins University.

ABBREVIATIONS: LA, local anesthetic; WT, wild-type; μ1, rat skeletal muscle Na^+ channels; hH1, human heart Na^+ channels; I-V, current-voltage; DIV, domain IV; g-V, conductance-voltage.

segment are known to affect activation (Planell-Cases et al., 1995; Seol et al., 1996; Li et al., 1998). We expanded our search to include the valine-to-isoleucine isoform variation (i.e., S4-V1451I), the only difference between the S4 segments of μ1 and hH1 channels, and other noncharged differences in DIV (i.e., F1342I and I1354F in S1, Y1379A in S2, and G1408S in S3; Fig. 1). We found that the isoform-specific leucine-to-glutamate difference in the S1/2 linker of domain IV (i.e., μ1-L1373E or hH1-E1555L) is an important determinant of the phenotypes of μ1 and hH1 Na^+ channels. Thus, the identification of the residue at this position plays a major role in shaping the responses of sodium channels to voltage and lidocaine, in part rationalizing the distinctive behavior of cardiac sodium channels.

Materials and Methods

Molecular Biology and Heterologous Expression. The gene encoding for the μ1 or hH1 sodium channel α-subunit was cloned into the pGFP-IRES vector with an internal ribosomal entry site separating it from the GFP reporter gene (Johns et al., 1997). Mutagenesis was performed in pGFP-IRES by using polymerase chain reaction with overlapping mutagenic primers. All mutations were made in duplicate and were confirmed by sequencing. Na^+ channel constructs were transfected into tsA-201 cells, which constitutively express t-antigen to boost the level of channel expression, by using LipofectAMINE Plus (Invitrogen, Carlsbad, CA) according to the manufacturer's protocol. Briefly, plasmid DNA encoding the wild-type (WT) or mutant α-subunit (1 μg/60-mm dish) was added to the cells with LipofectAMINE and was then incubated at 37°C in a humidified atmosphere of 95% O_2 and 5% CO_2 for 48 to 72 h before electrical recordings.

Electrophysiology. Electrophysiological recordings were performed at 21 to 22°C using the whole-cell, patch-clamp technique (Hamill et al., 1981) with pipettes having 1- to 3-MΩ tip resistance. Transfected cells were identified by their green epifluorescence during illumination at 488 ± 10 nM. The bath solution contained 140 mM NaCl, 5 mM KCl, 2 mM $CaCl_2$, 1 mM $MgCl_2$, 10 mM HEPES, and 10 mM glucose, with pH adjusted to 7.4 by the addition of NaOH. The pipette solution contained 35 mM NaCl, 105 mM CsF, 1 mM $MgCl_2$, 10 mM HEPES, and 1 mM EGTA, with pH adjusted to 7.2 by the addition of CsOH. Lidocaine was added to the bath solution at the concentrations indicated. A 5-min interval was allowed for equilibration whenever the drug concentration was changed. For channel-activation curves, only cells expressing peak currents of <3 nA were used to ensure proper voltage control. Series resistance was typically compensated at 50 to 60%.

Electrophysiological Protocols and Data Analysis. Current-voltage (I-V) relationships were recorded 5 to 10 min after the membrane rupture to minimize time-dependent activation shifts but allow enough time for the channels to equilibrate. Cells were initially held at −100 mV and were then increased to potentials from −80 to +50 mV incrementally. Steady-state activation curves were constructed using the equation $m_\infty = g/g_{max}$, where g was obtained from the I-V relationship by scaling the peak current (I) by the net driving force using the equation $g = I/(V_t - E_{rev})$. V_t is the test potential and V_{rev} is the reversal potential. Current-voltage data were fit to the equation $I = m_\infty \times g_{max} \times (V - E_{rev})$. Steady-state availability curves were obtained by normalizing the peak current recorded in test pulses to −20 mV for 50 ms after 500-ms prepulses to various voltages (−180 mV to −20 mV in 10-mV increments). Steady-state activation and inactivation curves were fit with the Boltzmann functions: m_∞ or $h_\infty = 1/(1 + \exp[(V_1 - V_{1/2})/k])$, where V_t is the test potential, $V_{1/2}$ is the half-point of the relationship, and k (= RT/zF) is the slope factor.

Use-dependent block was induced by applying a train of 100-ms step depolarizations to −10 mV from a holding potential of −100 mV at stimulation frequencies of 10, 5, 2, and 1 Hz in the absence or

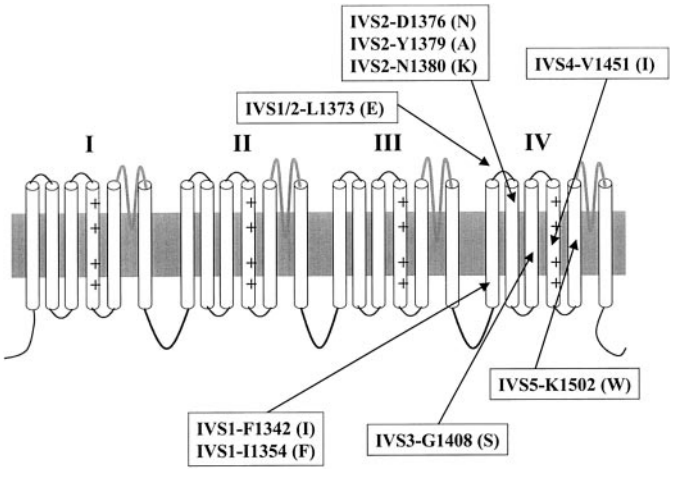

Fig. 1. Putative transmembrane topology of the Na^+ channel α-subunit showing the four internal homologous domains (DI-IV), each with six transmembrane segments (S1–6). μ1-Specific DIV residues were studied, and their approximate locations are indicated. Amino acids in parentheses indicate the corresponding residues at equivalent positions in the hH1 Na^+ channel isoform.

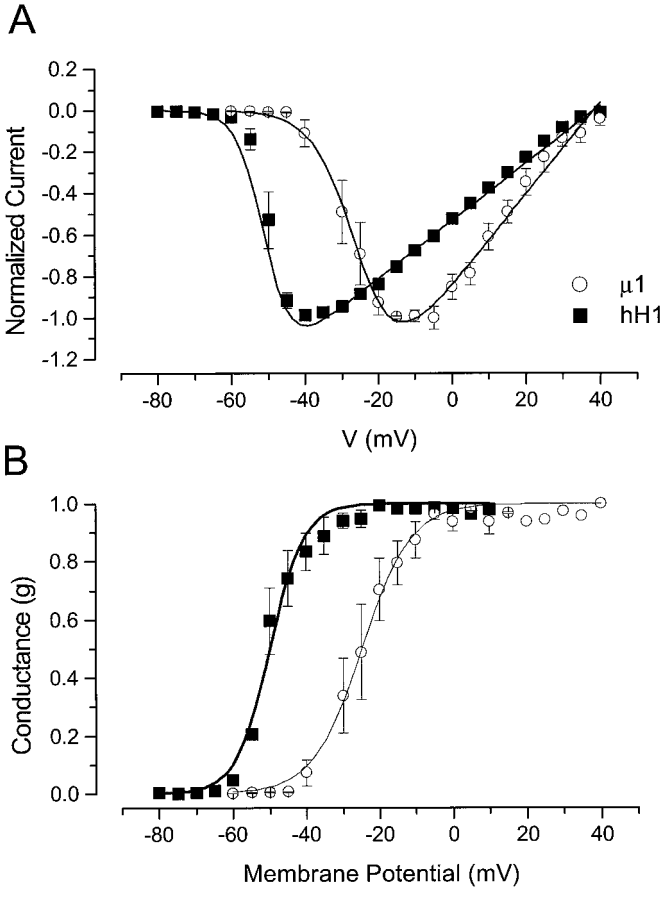

Fig. 2. Comparison of the I-V relationships and steady-state activation curves of the rat skeletal muscle (μ1) and human cardiac (hH1) Na^+ channels. A, the normalized peak I-V relationships of WT μ1 and hH1 channels. hH1 Na^+ channels open and close at more hyperpolarizing potentials than do the μ1 channels. B, steady-state activation curves derived from the corresponding I-V curves shown in A. A significant leftward shift of hH1 relative to μ1 was observed.

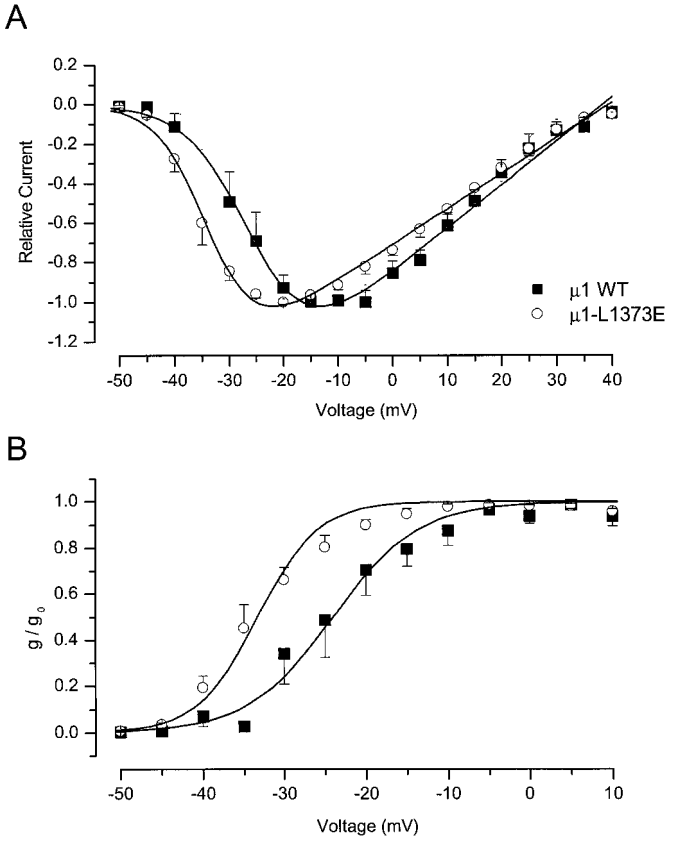

Fig. 3. Effects of isoform-specific mutations on the I-V relationship and steady-state activation curve of μ1 Na^+ channels. A, the normalized peak I-V relationships of WT μ1 and μ1-L1373E Na^+ channels. μ1-L1373E channels displayed a significant hyperpolarizing shift of the I-V curve relative to WT μ1 channels. B, steady-state activation curves derived from the I-V curves shown in A. The isoform-specific L1373E mutation caused a left-shift of the steady-state activation curve similar to that observed in the cardiac channels.

presence of lidocaine. The extent of steady-state, use-dependent block was assessed as the fraction of block of the 30th pulse compared with the first pulse [i.e., $1 - I_{pulse\ 30} / I_{pulse\ 1}$, where $I_{pulse\ 1}$ and $I_{pulse\ 30}$ represent the peak currents measured during the 1st and 30th pulses, respectively].

Data presented are the means ± S.E.M. Statistical significance was determined using Student's t test, with $p < 0.05$ representing significance.

Results

Comparison of Channel Activation of Wild-Type μ1 and hH1 Na^+ Channels. We first compared the I-V relationships of WT μ1 and hH1 Na^+ channels. Consistent with previous results (Nuss et al., 1995), the activation of hH1 channels was shifted ~20 mV in the hyperpolarizing direction compared with μ1 channels (Fig. 2A). This difference in activation was more evident after transforming these I-V relations into conductance-voltage (g-V) curves (Fig. 2B). The midpoints ($V_{1/2}$) and slope factors (k) estimated from these g-V curves were −27.4 ± 3.1 mV (n = 5) and 4.2 ± 0.7 (n = 5) and −46.9 ± 2.1 mV (n = 8) and 4.1 ± 1.3 (n = 8), respectively, for μ1 and hH1.

Effects of Isoform-Specific Amino Acid Differences on Channel Gating. As a first step toward probing the basis of the differences in gating, we converted isoform-specific amino acids in the S1/2 linker, S2, and S5 of domain IV in μ1 to their homologs in hH1 channels, focusing on residues whose side chains differ in charge (i.e., S1/2: L1373E; S2: D1376N/N1380K; and S5: K1502W; Fig. 2). All mutant channels except for K1502W expressed functional channels. The activation gating of L1373E channels shifted significantly ($p < 0.05$) so as to approximate that observed in WT hH1 channels (Fig. 3A); the double mutant D1376N/N1380K displayed a slight but statistically insignificant hyperpolarizing (leftward) shift compared with that of WT μ1 channels. These results suggest that the Leu-to-Glu charge difference located within the linker between the S1 and S2 segments partially underlies the differences in channel activation between the two channel isoforms. $V_{1/2}$ and k values of L1373E channels determined from the corresponding g-V curve (Fig. 2B) were −33.0 ± 1.4 mV (n = 9) and 4.5 ± 0.4 (n = 9), respectively.

In addition to the charge differences in domain IV, we also explored other noncharged amino acid differences within the same domain (Fig. 1). The relevant mutants were: S1-F1342I, S1-I1354F, S2-Y1379A, S3-G1408S, and S4-V1451I. None of these charge-neutral differences, however, affected the activation of μ1 (Table 1). For steady-state inactivation, V1451I channels displayed a hyperpolarizing shift (−74.2 ± 1.9 mV, n = 8) relative to WT μ1, whereas a depolarizing shift was observed with Y1379A channels (−55.4 ± 1.2 mV, n = 4). Others were not significantly different from WT ($p >$ 0.05). The steady-state gating parameters of all channels are summarized in Table 1. None of the mutant channels had

TABLE 1
Summary of steady-state gating parameters of Na^+ channels
Values are presented as mean ± S.E.M. Numbers in parentheses represent the number of individual determinations.

Channel	Activation (m_∞)		Inactivation (h_∞)	
	$V_{1/2}$	k	$V_{1/2}$	k
μ1	−27.4 ± 3.1 (5)	4.2 ± 0.7 (5)	−66.0 ± 1.3 (6)	6.4 ± 0.4 (6)
F1342I	−27.0 ± 2.3 (5)	4.9 ± 0.6 (5)	−66.9 ± 2.0 (4)	7.6 ± 0.4 (4)
I1354F	−27.05 ± 2.2 (3)	5.2 ± 0.6 (3)	−62.3 ± 1.0 (6)	7.7 ± 0.5 (6)
L1373E	−33.0 ± 1.4 (9)[a]	4.5 ± 0.4 (9)	−65.9 ± 2.9 (7)	7.9 ± 0.8 (7)
D1376N/N1380K	−30.6 ± 4.7 (3)	4.7 ± 0.6 (3)	−68.2 ± 2.6 (6)	7.4 ± 0.5 (6)
Y1379A	−29.9 ± 2.2 (3)	3.9 ± 0.3 (3)	−55.4 ± 1.2 (4)[a]	7.5 ± 0.3 (4)
G1408S	−25.7 ± 2.4 (7)	5.3 ± 0.4 (7)	−64.0 ± 1.6 (7)	8.0 ± 0.4 (7)
V1451I	−29.5 ± 2.6 (3)	4.3 ± 0.2 (3)	−74.2 ± 1.9 (8)[a]	7.3 ± 0.3 (8)
hH1	−46.9 ± 2.1 (8)[a]	4.1 ± 1.3 (8)	−83.9 ± 6.3 (4)[a]	6.3 ± 0.4 (4)[a]
hH1-E1555L	−35.8 ± 4.0 (7)[ab]	4.4 ± 0.5 (7)	−83.0 ± 5.6 (3)[a]	5.8 ± 0.4 (3)[a]

[a] Entries that are statistically different ($p < 0.05$) from wild-type μ1.
[b] hH1 construct statistically different from WT hH1 ($p < 0.05$).

reversal potentials (E_{rev}) that differed significantly from that of WT (data not shown).

hH1-E1555L Displayed Depolarizing Shift in Channel Activation. If μ1-L1373E genuinely plays a significant role in setting the isoform-specific differences in channel activation between μ1 and hH1, mutating the analogous glutamate in DIV-S1/2 of hH1 to the leucine of μ1 (i.e., E1555L) should shift the I-V relationship of hH1 channels in the opposite (depolarizing) direction. To test this prediction, we next studied hH1-E1555L. The I-V relationship of hH1-E1555L was indeed shifted in the depolarizing direction relative to WT hH1 channels; this single residue mutation very nearly reproduced the gating properties of μ1 (Fig. 4A). $V_{1/2}$ and k values estimated from the corresponding steady-state activation curve (Fig. 4B) were -35.8 ± 4.0 mV ($n = 7$) and 4.4 ± 0.5 ($n = 7$), respectively.

Effects of DIV Amino Acid Differences on Lidocaine Block. We next examined the effects of domain IV amino acid differences on use-dependent block by lidocaine by applying continuous trains of depolarizing pulses (see *Materials and Methods*). Figure 5 summarizes the steady-state use dependence (measured as $I_{Pulse\ 30}/I_{Pulse\ 1}$) of WT and mutated μ1 channels at different stimulation frequencies with or without 30 μM lidocaine. In the absence of drug, V1451I uniquely exhibited enhanced use-dependent current reduction at 5- and 10-Hz stimulation frequencies. In 30 μM lidocaine, both L1373E and V1451I channels displayed enhanced use-dependent drug block at 5 and 10 Hz relative to WT reactions (Fig. 5A). The noncharged mutant channels F1342I, I1354F, Y1379A, and G1408S exhibited use-dependence similar to that of WT μ1 under all conditions (data not shown). Although the enhanced use-dependent block of V1451I channels by lidocaine could be attributed to the greater intrinsic use-dependence in the absence of drug (Fig. 5A) and/or the negatively shifted steady-state availability curve (Table 1), such was not the case for L1373E channels; the enhanced use-dependent lidocaine block of this mutant cannot be ascribed to gating changes or differences in drug-free use dependence compared with WT μ1. To further investigate the role of this Leu-to-Glu difference, we examined the effect of the converse mutation hH1-E1555L on use-dependence of WT hH1 with 10 μM lidocaine. This drug concentration was chosen because it produces comparable levels of steady-state use-dependent block (~50%) of WT hH1 as 30

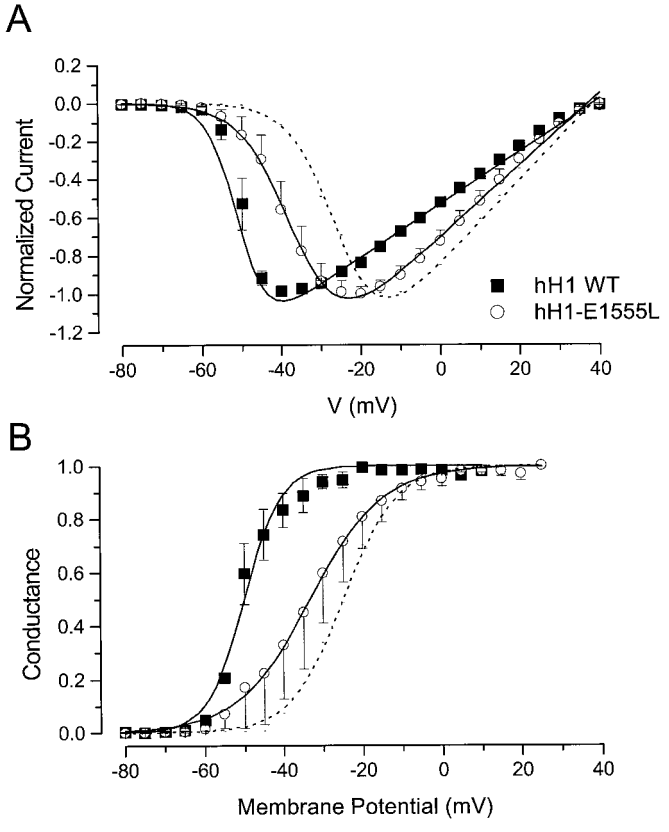

Fig. 4. Effects of hH1-E1555L on I-V and steady-state activation curves of hH1 Na^+ channels. A, normalized I-V relationships of WT hH1 (■) and hH1-E1555L (○) mutant channels. The I-V curve of E1555L was shifted in the same (depolarizing) direction as WT μ1 (broken line). B, steady-state activation plots of WT hH1 and hH1-E1555L mutant channels. Transformations of I-V relationships to steady-state activation curves were done as seen in Fig. 3.

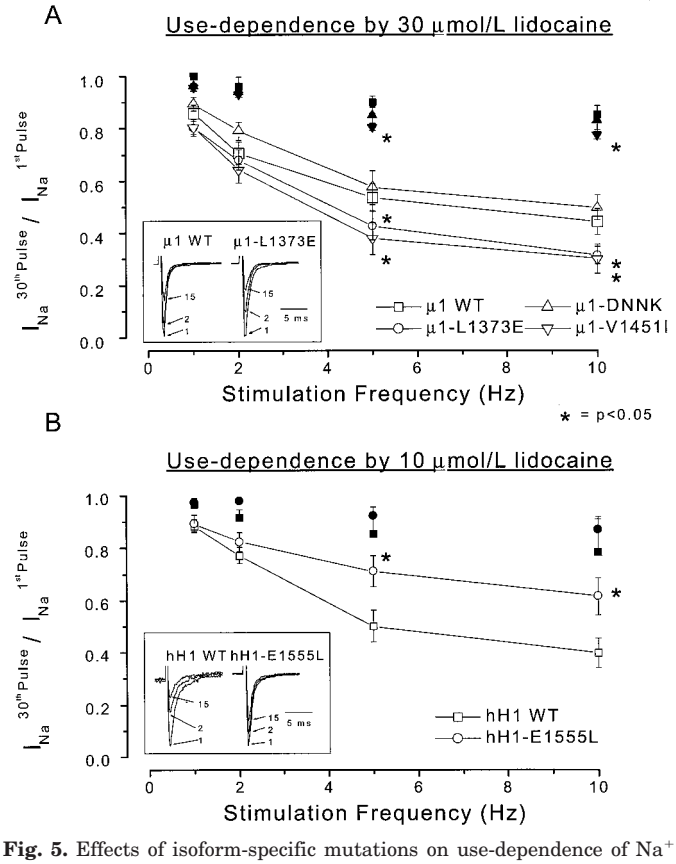

Fig. 5. Effects of isoform-specific mutations on use-dependence of Na^+ channels. A, plot of steady-state use dependence [measured as the ratio of peak Na^+ currents remaining at the 30th pulse to that measured during the 1st pulse (i.e., $I_{30th\ Pulse}/I_{1st\ Pulse}$)] of WT (squares), L1373E (circles), D1376N/N1380K (triangles) and V1451I (inverted triangles) Na^+ channels against stimulation frequency recorded in the absence (filled symbols) and presence (open symbols) of 30 μM lidocaine. Use-dependent current reduction by lidocaine was enhanced ($p < 0.05$) in the μ1-L1373E and μ1-V1451I mutant channels. The inset shows representative sodium currents through μ1 and μ1-L1373E channels recorded during the 1st, 2nd, and 30th pulses as indicated in the presence of 30 μM lidocaine when stimulated at 10 Hz at -10 mV from -100 mV. B, the effects of the converse mutation hH1-E1555L (circles) on the steady-state use dependence of WT hH1 (squares) Na^+ channels recorded with (open symbols) and without (filled symbols) 10 μM lidocaine. hH1-E1555L reduced use-dependent block of WT-hH1 by lidocaine. The inset shows representative current records of hH1 and hH1-E1555L channels during the 1st, 2nd, and 30th pulses measured with 10 μM lidocaine using the same voltage steps as used in A.

μM lidocaine does in WT μ1 channels (Fig. 5, A and B). Figure 5B shows that use-dependence of hH1-E1555L by 10 μM lidocaine was indeed reduced compared with WT hH1 at 5 and 10 Hz under identical conditions in the same direction as that observed in WT μ1. Changing the holding potentials from -100 mV to -120 mV did not alter this trend (Fig. 5). Thus, the identification of the residue at the isoform-variant hH1-E1555/μ1-L1373 position significantly influences both activation gating and LA use-dependent block. Despite changes in use dependence, hH1-E1555L and μ1-L1373E channels had resting-state (or tonic) block that was not different ($p > 0.05$) from that of the corresponding WT channels: e.g., at -10 mV, 1 mM lidocaine blocked μ1 and μ1-L1373E to 69.9 $\pm$ 3.5% ($n = 3$) and 63.3 $\pm$ 1.5% ($n = 3$) of the drug-free level, respectively. Similarly, 300 μM lidocaine blocked hH1 (67.6 $\pm$ 2.0%, $n = 3$) and hH1-E1555L (68.3 $\pm$ 5.5%, $n = 3$) to the same level. Holding potentials for these experiments were -140 mV and -180 mV for μ1 and hH1 channels, respectively, in which steady-state availability was nearly 100% for both channel isoforms (Nuss et al., 1995, 2000).

To address whether the changes in lidocaine response observed with μ1, μ1-L1373E, hH1, and hH1-E1555L channels were directly the result of their shifts in channel activation, we compared lidocaine-induced use-dependence of μ1 at -10 mV with μ1-L1373E at -20 mV and hH1 at -35 mV with hH1-E1555L at -20 mV (Fig. 6). These voltages were chosen because they were close to the corresponding I-V peaks of these channels and therefore should produce "equivalent" degrees of activation. The differences in drug sensitivity persisted even at these different test voltages. μ1-L1373E continued to display more prominent use-dependence than μ1, whereas hH1-E1555L channels were less sensitive than hH1.

Discussion

Na^+ channels from different tissues differ vastly in various functional and pharmacological properties. In particular, cardiac Na^+ channels activate at a greater number of negative membrane potentials and are more sensitive to local anesthetics than are their skeletal muscle and nerve counterparts (Nuss et al., 1995; Wang et al., 1996; Wright et al., 1997). Clinically, 5 to 20 μM lidocaine alters cardiac conduction by blocking Na^+ channels, whereas >100 μM is required to produce local anesthesia in nerve and skeletal muscle (Gianelly et al., 1967; Jewitt et al., 1968; Hille, 1978). Despite advances in our understanding of the general mechanisms of LA block of Na^+ channels, it remains controversial whether the enhanced drug sensitivity of the cardiac channels results from gating differences (Wright et al., 1997) or from an intrinsic difference in drug affinity (Nuss et al., 1995; Wang et al., 1996). In any case, the structural basis of isoform-specific differences in gating and drug sensitivity is poorly defined. To further complicate matters, gating processes in these channels are coupled so that isoform-specific differences may reflect differences in activation-inactivation coupling. Indeed, activation or slow inactivation, rather than fast inactivation itself, may underlie isoform-specific differences in LA action by virtue of the tight coupling between these processes (Armstrong and Bezanilla, 1977; Aldrich et al., 1983; Chahine et al., 1994; Chen et al., 1996; Yang et al., 1996; Nuss et al., 2000). We have found that site-specific differences in LA block persist even when voltage protocols are adjusted to produce "equivalent" degrees of activation. This fact indicates that the difference of activation voltage dependence does not suffice to explain the differences in LA between isoforms. Because inactivation is believed to derive its appar-

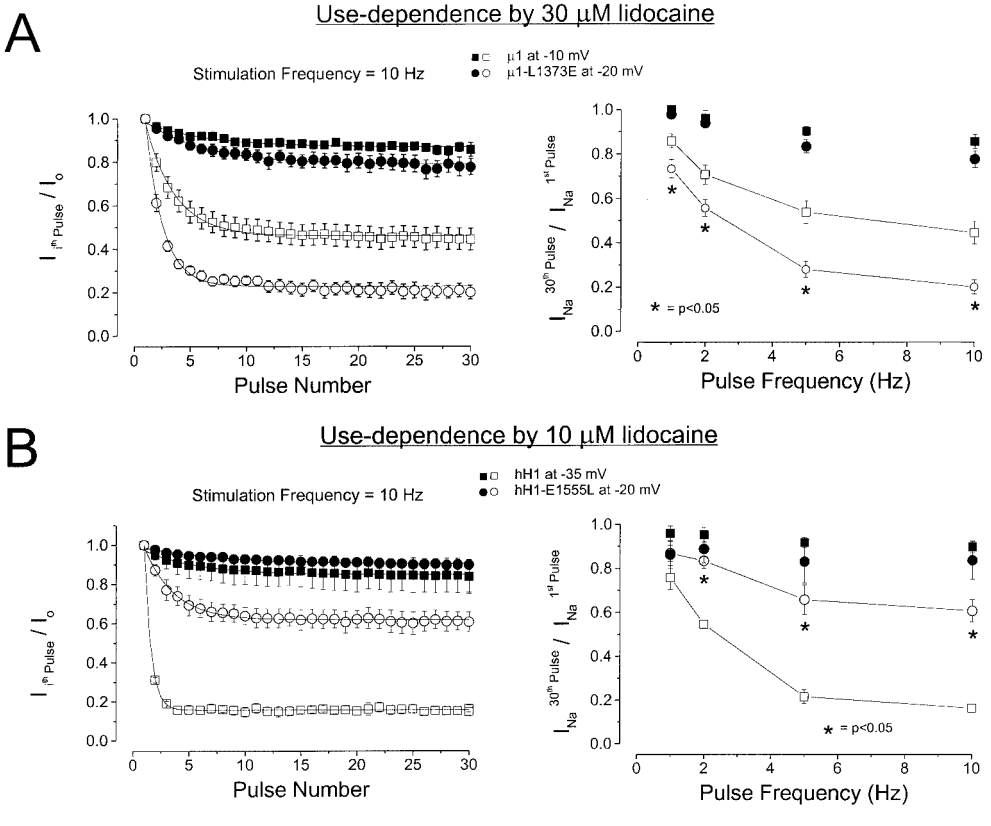

Fig. 6. Use-dependence at different activation voltages. A, left, time course of development of use-dependence of μ1 (squares) and μ1-L1373E (circles) channels in the absence (filled symbols) and presence (open symbols) of 30 μM lidocaine. Peak Na^+ currents were normalized to that measured during the first pulse and plotted against the pulse number. Use-dependence was induced by depolarizing channels to -10 for μ1 or -20 mV μ1-L1373E for 100 ms from rest at a holding potential of -100 mV at 10 Hz to adjust for their differences in activation. μ1-L1373E continued to display more prominent use-dependence than μ1. A, right, summary of steady-state use dependence ($I_{30th\ Pulse}/I_{1st\ Pulse}$) of μ1 and μ1-L1373E channels at other stimulation frequencies recorded using the same protocol. B, legends are the same as those shown in A but are for hH1 (squares) and hH1-E1555L (circles) Na^+ channels. Test voltages were -35 mV for hH1 and -20 mV for hH1-E1555L channels. Similar to μ1 and μ1-L1373E channels, the differences in drug sensitivity persisted at these different test voltages. Lidocaine (10 μM) was used in these experiments.

ent voltage dependence by being coupled to activation and activation but not inactivation was altered in L1373E (and hH1-E1555L) channels, this S1/2 variant residue seems to alter the coupling of the two gating processes. Therefore, our identification of novel isoform-specific determinants of gating and LA block should help to guide future studies directed at understanding the mechanistic links between the two processes.

The major finding of this study was the observation that substitution of the S1/2 linker residue L1373 in μ1 Na^+ channels with the glutamate found at the equivalent position in hH1 shifted activation in the hyperpolarizing direction and enhanced use-dependent block by lidocaine. These phenotypic changes rendered the skeletal muscle μ1 channels more "heart-like". The converse mutation in hH1 channels (i.e., E1555L) produced the opposite effects, making the heart channels more "muscle-like". Taken together, these results help rationalize the distinctive behavior of cardiac and skeletal muscle sodium channels. Our study addresses the basis of the intrinsic differences in lidocaine sensitivity between isoforms, but it should be noted that other factors, including differences in resting membrane potential, action potential duration, and action potential frequency in different tissues, can have critical effects on shaping drug action in vivo.

The transmembrane segments of Na^+ channels, as well as the cytoplasmic loops that interconnect them, are known to play important functional roles (e.g., protein phosphorylation, G-protein binding, channel activation, and inactivation); in contrast, little is known about the extracellular loops. In this study, we show that an external isoform variant (hH1-E1555) not only regulates activation but also modulates lidocaine block. Recently, we demonstrated that various P-S6 residues that were believed to be remote from major channel functional domains indeed shape the permeation phenotypes and also contribute significantly to Na^+ channel-specific μ-conotoxin binding (Li et al., 2000a,b). Other extracellular loops are also believed to participate in gating, binding of neurotoxins, and modulation by accessory subunits (Rogers et al., 1996; Cestele et al., 1998; Qu et al., 1999). Taken together, it is increasingly apparent that extracellular loops figure prominently in various functional properties of sodium channels.

References

Aldrich RW, Corey DP, and Stevens CF (1983) A reinterpretation of mammalian sodium channel gating based on single channel recording. *Nature (Lond)* **306:**436–441.

Armstrong CM and Bezanilla F (1977) Inactivation of the sodium channel. II. Gating current experiments. *J Gen Physiol* **70:**567–590.

Bennett ES (1999) Effects of channel cytoplasmic regions on the activation mechanisms of cardiac versus skeletal muscle Na^+ channels. *Biophys J* **77:**2999–3009.

Cestele S, Qu Y, Rogers JC, Rochat H, Scheuer T, and Catterall WA (1998) Voltage sensor-trapping: enhanced activation of sodium channels by beta-scorpion toxin bound to the S3–S4 loop in domain II. *Neuron* **21:**919–931.

Chahine M, George AL, Zhou M, Ji S, Sun W, Barchi RL, and Horn R (1994) Sodium channel mutations in paramyotonia congenita uncouple inactivation from activation. *Neuron* **12:**281–294.

Chen LQ, Santarelli V, Horn R, and Kallen RG (1996) A unique role for the S4 segment of domain 4 in the inactivation of sodium channels. *J Gen Physiol* **108:**549–556.

Courtney KR (1975) Mechanisms of frequency-dependent inhibition of sodium currents in frog myelinated nerve by the lidocaine derivative GEA 968. *J Pharmacol Exp Ther* **195:**225–236.

Gianelly R, van der Groeben JO, Spivack AP, and Harrison DC (1967) Effects of lidocaine on ventricular arrhythmias in patients with coronary heart diseases. *N Engl J Med* **277:**1215–1219.

Hamill OP, Marty A, Neher E, Sakmann B, and Sigworth FJ (1981) Improved patch-clamp techniques for high-resolution current recording from cells and cell-free membrane patches. *Pfleug Arch Eur J Physiol* **391:**85–100.

Hille B (1977) Local anesthetics: hydrophilic and hydrophobic pathways for the drug receptor reaction. *J Gen Physiol* **69:**479–515.

Hille B (1978) Local anesthetic action on inactivation of the Na^+ channel in nerve and skeletal muscle, in *Biophysical Aspects of Cardiac Muscle* (Morad M ed) pp 55–74, Academic Press Inc., New York.

Hondeghem LM and Katzung BG (1977) Time- and voltage-dependent interactions of anti-arrhythmic drugs with cardiac sodium channels. *Biochim Biophys Acta* **472:**373–398.

Jewitt DE, Kishon Y, and Thomas M (1968) Lidocaine in the management of arrhythmias after acute myocardial infarction. *Lancet* **1:**266–270.

Johns DC, Nuss HB, and Marban E (1997) Suppression of neuronal and cardiac transient outward currents by viral gene transfer of dominant-negative Kv4.2 constructs. *J Biol Chem* **272:**31598–31603.

Li RA, Ennis IL, Velez P, Tomaselli GF, Marban E (2000a) Novel structural determinants of μ-conotoxin (GIIIB) block in rat skeletal muscle (μ1) Na^+ channels. *J Biol Chem* **275:**27551–27558.

Li RA, Tsushima RG, and Backx PH (1998) Highly conserved residues in the S3 segments of rat skeletal muscle Na^+ channel play a role in channel activation and inactivation. *Biophys J* **72:**B2.

Li RA, Velez P, Chiamvimonvat N, Tomaselli GF, Marbán E (2000b) Charged residues between selectivity filter and S6 segments contribute to the permeation phenotype of the sodium channel. *J Gen Physiol* **115:**81–92.

Makielski JC, Limberis J, Fan Z, and Kyle JW (1999) Intrinsic lidocaine affinity for Na channels expressed in *Xenopus* oocytes depends on alpha (hH1 vs. rSkM1) and beta 1 subunits. *Cardiovasc Res* **42:**503–509.

Nuss HB, Kambouris NG, Marban E, Tomaselli GF, Balser JR (2000) Isoform-specific lidocaine block of sodium channels explained by differences in gating. *Biophys J* **78:**200–210.

Nuss HB, Tomaselli GF, and Marban E (1995) Cardiac sodium channels (hH1) are intrinsically more sensitive to block by lidocaine than are skeletal muscle (μ1) channels. *J Gen Physiol* **106:**1193–1209.

Planell-Cases R, Ferrer-Montiel AV, Patten CD, and Montal M (1995) Mutation of conserved negatively charged residues in the S2 and S3 transmembrane segments of a mammalian K^+ channel selectively modulates channel gating. *Proc Natl Acad Sci USA* **92:**9422–9426.

Qu Y, Rogers JC, Chen SF, McCormick KA, Scheuer T, and Catterall WA (1999) Functional roles of the extracellular segments of the sodium channel alpha subunit in voltage-dependent gating and modulation by beta1 subunits. *J Biol Chem* **274:**32647–32654.

Ragsdale DS, McPhee JC, Scheuer T, and Catterall WA (1994) Molecular determinants of state-dependent block of Na^+ channels by local anesthetics. *Science (Wash DC)* **265:**1724–1728.

Ragsdale DS, McPhee JC, Scheuer T, and Catterall WA (1996) Common molecular determinants of local anesthetic, antiarrhythmic and anticonvulsant block of voltage-gated Na^+ channels. *Proc Natl Acad Sci USA* **93:**9270–9275.

Rogers JC, Qu Y, Tanada TN, Scheuer T, and Catterall WA (1996) Molecular determinants of high affinity binding of alpha-scorpion toxin and sea anemone toxin in the S3–S4 extracellular loop in domain IV of the Na+ channel alpha subunit. *J Biol Chem* **271:**15950–15962.

Seol SA, Sigg D, Papazian DM, and Bezanilla F (1996) Voltage-sensing residues in the S2 and S4 segments of the Shaker K^+ channel. *Neuron* **16:**1159–1167.

Sigworth FJ (1993) Voltage gating of ion channels. *Q Rev Biophys* **27:**1–40.

Stühmer W, Conti F, Suzuki H, Wang X, Noda M, Yahagi N, Kubo H, and Numa S (1989) Structural parts involved in activation and inactivation of the sodium channel. *Nature (Lond)* **339:**597–603.

Wang DW, Li N, George AL, and Bennett PB (1996) Distinct local anesthetic affinities in Na^+ channel subtypes. *Biophys J* **70:**1700–1708.

Wright SN, Wang SY, Kallen RG, and Wang GK (1997) Differences in steady-state inactivation between Na channel isoforms affect local anesthetic binding affinity. *Biophys J* **73:**779–788.

Yang N, George AL, and Horn R (1996) Molecular Basis of charge movement in voltage-gated sodium channels. *Neuron* **16:**113–122.

Zhang Y, Hartmann HA, and Satin J (1999) Glycosylation influences voltage-dependent gating of cardiac and skeletal muscle sodium channels. *J Membr Biol* **171:**195–207.

Address correspondence to: Eduardo Marbán, M.D., Ph.D., Institute of Molecular Cardiobiology, The Johns Hopkins University School of Medicine, 720 Rutland Avenue/Ross 844, Baltimore MD 21205. E-mail: marban@jhmi.edu